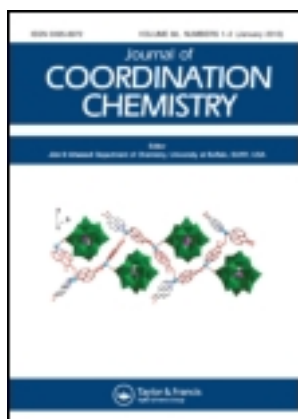


This article was downloaded by: [Moskow State Univ Bibliote]

On: 14 December 2013, At: 23:20

Publisher: Taylor & Francis

Informa Ltd Registered in England and Wales Registered Number: 1072954 Registered office: Mortimer House, 37-41 Mortimer Street, London W1T 3JH, UK



Journal of Coordination Chemistry

Publication details, including instructions for authors and subscription information:

<http://www.tandfonline.com/loi/gcoo20>

Tetradentate N_2O_2 type Nickel(II) Schiff base complexes derived from meso-1,2-diphenyle-1,2-ethylenediamine: synthesis, characterization, crystal structures, electrochemistry, and catalytic studies

Mahsa Pooyan^a, Abolfazl Ghaffari^a, Mahdi Behzad^a, Hadi Amiri Rudbari^b & Giuseppe Bruno^c

^a Department of Chemistry, Semnan University, Semnan, Iran

^b Faculty of Chemistry, University of Isfahan, Isfahan, Iran

^c Università degli Studi di Messina, dip. Scienze Chimiche. Viale Ferdinando S. d'Alcontres, Messina, Italy

Published online: 10 Dec 2013.

To cite this article: Mahsa Pooyan, Abolfazl Ghaffari, Mahdi Behzad, Hadi Amiri Rudbari & Giuseppe Bruno (2013) Tetradentate N_2O_2 type Nickel(II) Schiff base complexes derived from meso-1,2-diphenyle-1,2-ethylenediamine: synthesis, characterization, crystal structures, electrochemistry, and catalytic studies, Journal of Coordination Chemistry, 66:24, 4255-4267, DOI: [10.1080/00958972.2013.867031](https://doi.org/10.1080/00958972.2013.867031)

To link to this article: <http://dx.doi.org/10.1080/00958972.2013.867031>

PLEASE SCROLL DOWN FOR ARTICLE

Taylor & Francis makes every effort to ensure the accuracy of all the information (the "Content") contained in the publications on our platform. However, Taylor & Francis, our agents, and our licensors make no representations or warranties whatsoever as to the accuracy, completeness, or suitability for any purpose of the Content. Any opinions and views expressed in this publication are the opinions and views of the authors, and are not the views of or endorsed by Taylor & Francis. The accuracy of the Content should not be relied upon and should be independently verified with primary sources of information. Taylor and Francis shall not be liable for any losses, actions, claims, proceedings, demands, costs, expenses, damages, and other liabilities whatsoever or howsoever caused arising directly or indirectly in connection with, in relation to or arising out of the use of the Content.

This article may be used for research, teaching, and private study purposes. Any substantial or systematic reproduction, redistribution, reselling, loan, sub-licensing, systematic supply, or distribution in any form to anyone is expressly forbidden. Terms & Conditions of access and use can be found at <http://www.tandfonline.com/page/terms-and-conditions>

Tetradentate N₂O₂ type Nickel(II) Schiff base complexes derived from *meso*-1,2-diphenyle-1,2-ethylenediamine: synthesis, characterization, crystal structures, electrochemistry, and catalytic studies

MAHSA POOYAN[†], ABOLFAZL GHAFARI[†], MAHDI BEHZAD^{*†},
HADI AMIRI RUDBARI[‡] and GIUSEPPE BRUNO[§]

[†]Department of Chemistry, Semnan University, Semnan, Iran

[‡]Faculty of Chemistry, University of Isfahan, Isfahan, Iran

[§]Università degli Studi di Messina, dip. Scienze Chimiche. Viale Ferdinando S. d'Alcontres, Messina, Italy

(Received 7 September 2013; accepted 14 November 2013)

A series of Ni(II) complexes of salen type Schiff base ligands were synthesized and characterized. The ligands were synthesized from the condensation of *meso*-1,2-diphenyle-1,2-ethylenediamine with salicylaldehyde (H₂L¹), 5-bromosalicylaldehyde (H₂L²), 5-bromo-3-nitrosalicylaldehyde (H₂L³), and 2'-hydroxyacetophenone (H₂L⁴). The complexes were characterized by means of ¹HNMR, IR, and UV-Vis spectroscopy and elemental analysis. Crystal structures of NiL³ and NiL⁴ were also determined by x-ray crystallography. Electrochemistry of the complexes was studied by means of cyclic voltammetry. Catalytic performance of the complexes was studied in the oxidation of cyclooctene using *tert*-butylhydroperoxide (TBHP) as oxidant. Various factors including solvent type, reaction temperature, time, catalyst amount, and substrate to oxidant ratio were optimized. Solvent free oxidation of cyclooctene with these catalysts was also studied. Increased catalytic activity and higher epoxide selectivity was achieved in solvent-free conditions. NiL⁴ with more electron donating substituents on the ligand was the most efficient oxidation catalyst.

Keywords: Schiff base; Nickel(II); Crystal structure; Epoxidation; Cyclooctene

1. Introduction

Fine tuning the electronic and steric properties of transition metal complexes to control the redox properties and catalytic activity of these compounds has been the subject of several studies [1–5]. In this regard, Schiff base ligands have obtained considerable attention, since the steric and electronic effects on these ligands could be easily achieved by the possibility of the introduction of various substituents on both the amine and the carbonyl moieties [6–8, 10]. Transition metal complexes of salen type tetradentate Schiff base ligands have been shown to catalyze various industrially and laboratory important reactions such as polymerization, ring opening polymerization, oxidation, reduction, alkylation reactions, etc. [11–15]. Epoxidation of olefins is a pivotal reaction in organic chemistry [16–30]. Perhaps,

*Corresponding author. Emails: mbehzad@semnan.ac.ir; mahdibehzad@gmail.com

the most celebrated complex in such studies is Jacobsen's catalyst, which has been shown to achieve high enantioselectivity in epoxidation of alkenes [14]. Nickel(II) complexes of tetradentate salen type Schiff base ligands have also been investigated in both homogenous and heterogeneous epoxidation of alkenes [17–20]. Besides, almost all of the usual epoxidation of alkenes are performed in organic solvents and solvent free conditions have not received necessary attention. Herein, and in continuation of our previous studies on the factors affecting the transition metal Schiff base-catalyzed epoxidation of alkenes [21–24], we report the synthesis, characterization, crystal structures, and catalytic performances of a series of nickel(II) complexes of salen type Schiff base ligands in the epoxidation of cyclooctene. The Schiff bases were synthesized from the condensation of *meso*-1,2-diphenyl-1,2-ethylenediamine with salicylaldehyde (H_2L^1), 5-Bromosalicylaldehyde (H_2L^2), 5-bromo-3-nitrosalicylaldehyde (H_2L^3), and 2'-hydroxyacetophenone (H_2L^4). The nickel(II) central ion was deliberately chosen since we are studying the epoxidation of cyclooctene with similar ligands but different metal ions to find the factors governing the reactivity of such complexes due to the presence of different electronic and steric factors of the central metal ion. The complexes were tested as catalysts in the oxidation of cyclooctene with *tert*-butylhydroperoxide (TBHP) under various conditions to find the optimum operating conditions. Moderate catalytic activity and epoxide selectivity was achieved. Solvent free epoxidation of cyclooctene with these catalysts was also studied. The catalysts showed increased activity and higher epoxide selectivity in the solvent-free conditions. NiL^4 with more electron donating substituents on the ligand was the most efficient oxidation catalyst.

2. Experimental

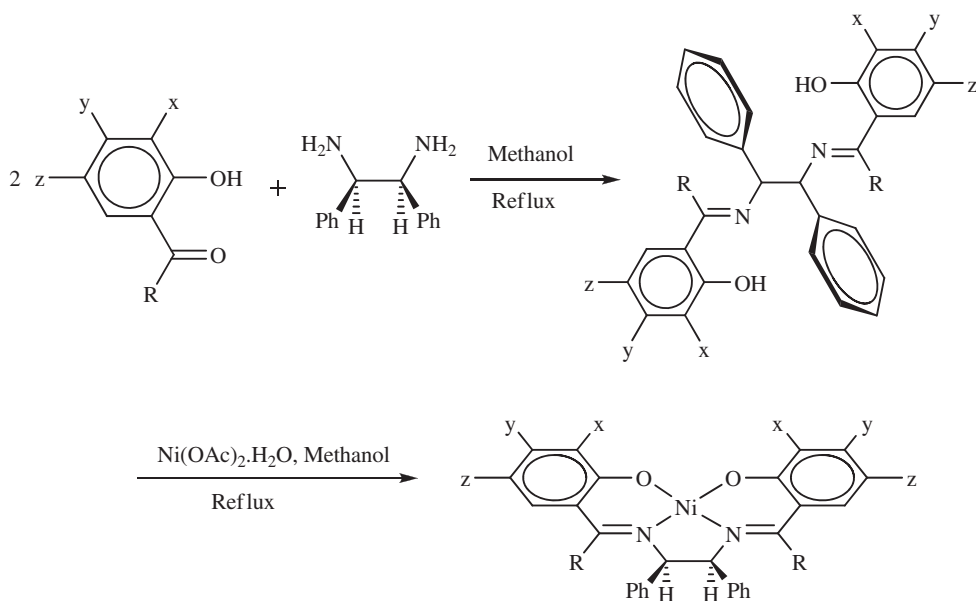
2.1. Materials and methods

All chemicals were purchased from commercial sources and were used as received. *Meso*-1,2-diphenyl-1,2-ethylenediamine [31] and the H_2L^x ($x = 1-3$) ligands were synthesized as described elsewhere [21, 22]. H_2L^4 was also synthesized following a similar procedure. Melting points were obtained on a thermoscientific 9100 apparatus. Elemental analyses were performed using a Perkin-Elmer 2400II CHNS-O elemental analyzer. 1H NMR spectra were recorded on a 500MHz Bruker FT-NMR spectrometer using $CDCl_3$ or $DMSO-d_6$ as solvent; chemical shifts (δ) are given in ppm. IR spectra were obtained as KBr plates using a Bruker FT-IR instrument. UV-Vis spectra were obtained on a Shimadzu UV-1650PC spectrophotometer in DMSO solutions. A Metrohm 757 VA computerized instrument was employed to obtain cyclic voltammograms. X-ray data were collected at room temperature with a Bruker APEX II CCD area-detector diffractometer using Mo $K\alpha$ radiation ($\lambda = 0.71073\text{\AA}$). Gas chromatography (GC) analyses were carried out on a GC-17A Shimadzu instrument.

2.2. Synthesis of the ligands

2.2.1. Synthesis of H_2L^4 . The ligands were readily synthesized by the reaction between methanolic solutions of 1 equivalent of *meso*-1,2-diphenyl-1,2-ethylenediamine and 2 equivalent of the appropriate carbonyl compound (scheme 1). In a typical experiment and for the

synthesis of the new derivative, H_2L^4 , 20 mL of a methanolic solution of *meso*-1,2-diphenyl-1,2-ethylenediamine (1 mM, 0.21 g) was placed in a round-bottom two-necked flask equipped with a reflux condenser, a dropping funnel, and a magnetic stirrer. This solution was stirred vigorously and heated to reflux and then from the dropping funnel was added a solution of 2 mM (0.27 g) 2'-hydroxyacetophenone in 10 mL of methanol and the reaction mixture was heated at reflux for a further 3 h during which the color of the solution gradually turned yellow. The progress of the reaction was checked by TLC. The reaction mixture was then left undisturbed overnight to yield a yellow powder, which was recrystallized from THF to give 0.33 g of yellow crystals of the target compound (73.2%). M.P. = 243 °C. Selected IR (KBr, cm^{-1}): 3460 (ν_{O-H}), 1608 ($\nu_{C=N}$). 1H NMR (δ , ppm): 15.73 (2H, s, OH), 7.51–6.69 (18H, m, H_{Ar}), 5.52 (2H, s, CHPh), 2.13 (6H, s, CH_3). UV–Vis in DMSO: λ ,



Ligands and Complexes	R	x	y	z
H_2L^1, NiL^1	H	H	H	H
H_2L^2, NiL^2	H	H	H	Br
H_2L^3, NiL^3	H	NO_2	H	Br
H_2L^4, NiL^4	CH_3	H	H	H

Scheme 1. Synthetic procedure for the ligands and complexes.

nm; (ϵ , $M^{-1} \text{ cm}^{-1}$): 261 (~85000), 323 (~15800). Anal. Calcd for $C_{30}H_{28}N_2O_2$: C, 80.36; H, 6.25; N, 6.25. Found: C, 80.23; H, 6.31; N, 6.20.

2.3. Synthesis of the complexes

The complexes were synthesized following a similar procedure as described elsewhere for NiL^1 (scheme 1) [32].

2.3.1. Synthesis of NiL^2 .DMF. In a typical experiment, a solution of 0.58 g (1 mM) of H_2L^2 in 30 mL of methanol was placed in a round bottom two-necked flask equipped with a magnetic stirrer, a dropping funnel and a condenser. This solution was heated to about 60 °C while being vigorously stirred and then a solution of 0.19 g $Ni(OAc)_2 \cdot H_2O$ (1mM) in 30 mL of methanol was added drop-wise from the dropping funnel. The color of the solution gradually turned red. The reaction mixture was heated for 3 h and then it was left undisturbed overnight. The resulting precipitate was filtered, washed with 10 mL of methanol and air dried. Recrystallization from DMF yielded red crystals of the target compound. Attempts to prepare single crystals of this compound failed. Yield: 0.56 g (88%). 1H NMR (δ , ppm): 7.63 (2H, s, $HC=N$); 7.426.70 (m, 16H, H_{Ar}); 5.08 (s, 2H, $CHPh$). Selected IR (KBr, cm^{-1}): 2920–3070 (ν_{C-H}), 1612 ($\nu_{C=N}$), 1519 ($\nu_{C=C}$), 1184 (ν_{C-O}). UV-Vis in DMSO: λ , nm; (ϵ , $M^{-1} \text{ cm}^{-1}$): 260 (~60600), 339 (~7700), 366 (~4400), 432 (~5400), 470 (~2000), 550 (~220). Anal. Calcd for $C_{31}H_{27}Br_2N_3NiO_3$: C, 52.58; H, 3.84; N, 5.93. Found: C, 52.62; H, 3.90; N, 5.89.

2.3.2. Synthesis of NiL^3 .DMF. This complex was synthesized following a similar procedure as described for NiL^2 except H_2L^3 was used instead of H_2L^2 . Recrystallization from DMF gave red single crystals of the target complex suitable for x-ray crystallography. 1H NMR (δ , ppm): 7.37 (2H, s, $HC=N$); 7.30–6.91 (m, 14H, H_{Ar}); 4.88 (s, 2H, $CHPh$). Selected IR (KBr, cm^{-1}): 2900–3070 (ν_{C-H}), 1616 ($\nu_{C=N}$), 1527 ($\nu_{C=C}$), 1195 (ν_{C-O}). UV-Vis in DMSO: λ , nm; (ϵ , $M^{-1} \text{ cm}^{-1}$): 258 (~55300), 342 (~7100), 430 (~8300), 452 (~7200), 544 (~230). Anal. Calcd for $C_{31}H_{25}Br_2N_5NiO_7$: C, 46.61; H, 3.13; N, 8.77. Found: C, 46.70; H, 3.18; N, 8.68.

2.3.3. Synthesis of NiL^4 .2CHCl₃. This complex was also synthesized following a similar procedure as described for NiL^2 except H_2L^4 was used instead of H_2L^2 . Recrystallization from chloroform gave single crystals of the target complex suitable for x-ray crystallography. 1H NMR (δ , ppm): 7.78–6.45 (m, 18H, H_{Ar}); 5.00 (s, 2H, $CHPh$), 2.10 (s, 6H, CH_3). Selected IR (KBr, cm^{-1}): 2900–3070 (ν_{C-H}), 1598 ($\nu_{C=N}$), 1560–1527 ($\nu_{C=C}$), 1164 (ν_{C-O}). UV-Vis in DMSO: λ , nm; (ϵ , $M^{-1} \text{ cm}^{-1}$): 262 (~61700), 333 (~10700), 414 (~9900), 450 (~5000), 547 (~400). Anal. Calcd for $C_{32}H_{28}Cl_6N_2NiO_2$: C, 51.61; H, 3.76; N, 3.76. Found: C, 51.68; H, 3.80; N, 3.70.

2.4. X-ray crystallography

Diffraction data were collected at room temperature with a Bruker APEX II CCD area-detector diffractometer using Mo $K\alpha$ radiation ($\lambda = 0.71073 \text{ \AA}$). Data collections, cell refinements, data reductions, and absorption corrections were performed using multi-scan

Table 1. Crystal data, data collection and structure refinement parameters for NiL³ and NiL⁴.

Compound	NiL ³	NiL ⁴
Empirical formula	C ₃₁ H ₂₅ Br ₂ N ₅ NiO ₇	C ₃₂ H ₂₈ Cl ₆ N ₂ NiO ₂
Formula weight	798.09	743.97
Temperature (K)	298(2)	298(2)
λ (Å)	0.71073	0.71073
Crystal system	Triclinic	Monoclinic
space group	<i>P</i> -1	<i>P</i> 2 ₁ / <i>c</i>
Unit cell dimensions (Å, °)		
<i>a</i> (Å)	10.4565(7)	14.3642(3)
<i>b</i> (Å)	11.4382(7)	9.4268(2)
<i>c</i> (Å)	14.5234(9)	23.9211(3)
α , °	72.446(3)	90.00
β , °	69.185(3)	96.906(5)
γ , °	83.042(3)	90.00
Volume (Å ³), <i>Z</i>	1547.88(17), 2	3215.62(10), 4
Calculated density (Mg m ⁻³)	1.712	1.537
Absorption coefficient (mm ⁻¹)	3.265	1.135
<i>F</i> (000)	800	1520
θ Range for data collection (°)	2.07 to 26.00	2.32 to 26.00
Limiting indices	-12 ≤ <i>h</i> ≤ 12, -14 ≤ <i>k</i> ≤ 14, -17 ≤ <i>l</i> ≤ 17	-17 ≤ <i>h</i> ≤ 17, -11 ≤ <i>k</i> ≤ 11, -29 ≤ <i>l</i> ≤ 29
Data/restraints/parameters	6070/0/415	6312/0/391
Total reflections	52518	99703
Unique reflections (<i>R</i> _{int})	6070 (0.1127)	6312 (0.1185)
Completeness	99.9%	99.9%
Refinement method	Full-matrix least-squares on <i>F</i> ²	Full-matrix least-squares on <i>F</i> ²
Goodness-of-fit on <i>F</i> ²	0.969	1.057
Final <i>R</i> index [<i>I</i> > 2 σ (<i>I</i>)]	<i>R</i> ₁ = 0.0396, <i>wR</i> ₂ = 0.1143	<i>R</i> ₁ = 0.0826, <i>wR</i> ₂ = 0.2198
<i>R</i> index [all data]	<i>R</i> ₁ = 0.0472, <i>wR</i> ₂ = 0.1203	<i>R</i> ₁ = 0.1018, <i>wR</i> ₂ = 0.2434
Largest difference peak and hole (e Å ⁻³)	0.711 and -0.580	1.581 and -0.773

methods with Bruker software [33]. The structures were solved by direct methods using SIR2004 [34]. The non-hydrogen atoms were refined anisotropically by the full matrix least squares method on *F*² using SHELXL [35]. All the hydrogen (H) atoms were placed at the calculated positions and constrained to ride on their parent atoms. Details concerning collections and analyses are reported in table 1.

2.5. Cyclic voltammetry

A Metrohm 757 VA computerized instrument was employed to obtain cyclic voltammograms in DMSO solutions at room temperature (25 °C) under nitrogen atmosphere using 0.1 M tetra-*n*-octylammonium bromide (TOAB) as supporting electrolyte. A platinum working electrode, a platinum auxiliary electrode and an Ag/AgCl reference electrode was used to obtain cyclic voltammograms.

2.6. General oxidation reactions

2.6.1. In-solvent oxidation of cyclooctene.

These Nickel(II) Schiff base complexes were used as catalysts for oxidation of cyclooctene using TBHP as oxidant in different solvents and various reaction conditions. The progress of the reaction was monitored by GC in 30 min intervals. The retention times for the starting materials and the products were

determined by comparison with authentic samples. In the absence of the complexes, no or very few oxidation products were observed. Oxidation of cyclooctene gave cycloocteneoxide as the major product of the reaction. The conversion percentages (%) and the TONs were calculated by the following equations, in which C_i and C_f are initial and final concentration of the substrate, respectively, and $[Q]$ is the concentration of the catalyst. In a typical experiment, 10 μM of NiL^4 catalyst was dissolved in 10 mL of freshly distilled acetonitrile and then 15 mM of cyclooctene and 30 mM of TBHP were added. The reaction mixture was refluxed while being stirred and the reaction progress was monitored at 30 min intervals.

$$\text{Conversion (\%)} = [(C_i - C_f) \times 100]/C_i \quad (1)$$

$$\text{Turn over number (TON)} = [(\% \text{Conversion}) \times C_i]/[Q] \quad (2)$$

2.6.2. Solvent free oxidations. Typically, a mixture of 15 μM of the catalysts, 15 mM of cyclooctene, and 45 mM of TBHP were refluxed and the progress of the reaction was monitored every 30 min by GC.

3. Results and discussions

3.1. Spectroscopic characterizations

In the IR spectra of the previously reported ligands (H_2L^{1-3}) [23] and the new H_2L^4 ligand, the presence of an intense band at around $1610 \pm 10 \text{ cm}^{-1}$ was assigned to the stretching vibration of the C=N group. This band was present in the IR spectra of the complexes but had shifted to lower wave numbers upon coordination, indicating that the nitrogen atoms of the imine groups had participated in coordination. The electronic absorption spectra of H_2L^4 showed two intense bands at 261 and 323 nm corresponding to the $\pi \rightarrow \pi^*$ transitions of the phenyl rings and azomethine groups, respectively [32]. These peaks were present in the electronic absorption spectra of the complexes. The red shift of the latter band ($\pi \rightarrow \pi^*$ transitions of the C=N groups) further confirmed the coordination of the nitrogen atoms of the azomethine groups. The electronic absorption spectra of the complexes showed a band at around $420 \pm 10 \text{ nm}$ with a shoulder at higher wavelengths which could be assigned to the LMCT comprised of a transition between the metal centered HOMO to the ligand centered LUMO ($\text{C}=\text{N}(\pi^*)$) [23]. The weak bands at about 545 nm are also assignable to the d-d transitions. In the ^1H NMR spectra of the ligands, the presence of broad (br) bands at above 13 ppm was assigned to the presence of phenolic protons. These signals were absent in the ^1H NMR spectra of NiL^x complexes, which meant that the quadridentate H_2L^x ligands were doubly deprotonated at the phenolate oxygen atoms [21–23]. The azomethine protons of the free Schiff base ligands (H_2L^{1-3}) gave sharp singlet signals (s) at around 8 ppm, which were shifted up-field to about $7.50 \pm 0.15 \text{ ppm}$ in the diamagnetic nickel(II) complexes. This observation was indicative of the incorporation of the nitrogen atoms of the azomethine groups in coordination to the Ni(II) center. Other signals, which appeared as multiplets (m) in the aromatic region at around 6.50 to 7.50, could be assigned to the aromatic protons of the Schiff base ligands. Aliphatic protons of the diamine part of the Schiff base ligands appeared at around 5 ppm with appropriate signal intensity. A sharp singlet

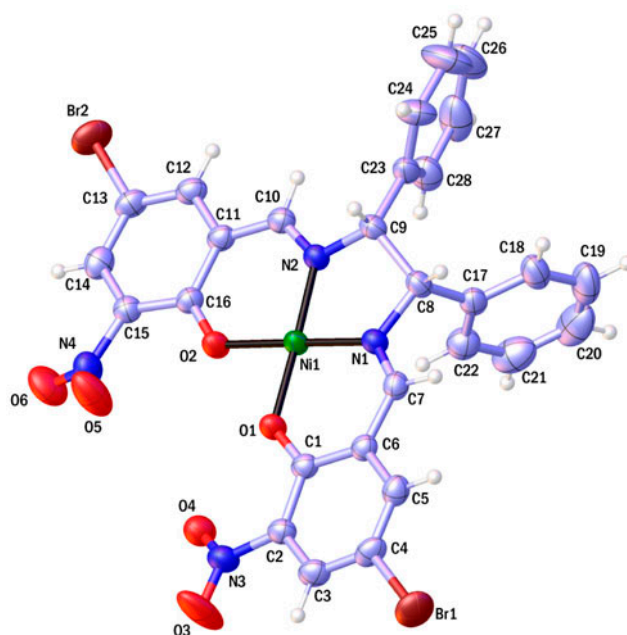


Figure 1. ORTEP representation of $\text{NiL}^3 \cdot \text{DMF}$. Thermal ellipsoids are drawn at the 50% probability level, while the hydrogen size is arbitrary. Solvent (DMF) has been omitted for clarity.

Table 2. Selected bond lengths and angles for NiL^3 and NiL^4 .

Complex	Selected bond lengths (Å)		Selected bond angles (°)	
NiL^3	Ni(1)–O(1)	1.8467(17)	O(1)–Ni(1)–O(2)	84.54(7)
	Ni(1)–O(2)	1.8496(16)	O(1)–Ni(1)–N(1)	94.56(8)
	Ni(1)–N(1)	1.833(2)	O(2)–Ni(1)–N(1)	178.90(8)
	Ni(1)–N(2)	1.842(2)	O(1)–Ni(1)–N(2)	177.59(9)
NiL^4			O(2)–Ni(1)–N(2)	94.74(8)
	Ni(1)–O(1)	1.823(4)	N(1)–Ni(1)–N(2)	86.13(9)
	Ni(1)–O(2)	1.818(4)	O(1)–Ni(1)–O(2)	82.35(19)
	Ni(1)–N(1)	1.872(5)	O(1)–Ni(1)–N(1)	95.17(19)
	Ni(1)–N(2)	1.859(4)	O(2)–Ni(1)–N(1)	172.7(2)
			O(1)–Ni(1)–N(2)	174.3(2)
			O(2)–Ni(1)–N(2)	93.95(19)
			N(1)–Ni(1)–N(2)	89.0(2)

signal was observed at 2.10 ppm for NiL^4 due to CH_3 protons, which had also been seen in the same region for H_2L^4 . Elemental analysis also confirmed the synthesis of the H_2L^4 ligand and the complexes.

3.2. Description of the crystal structures

3.2.1. Description of the crystal structure of NiL^3 . Red crystals of NiL^3 suitable for X-ray crystallography were obtained by recrystallization from a DMF solution after one week. An ORTEP drawing of this compound is shown in figure 1 along with a common

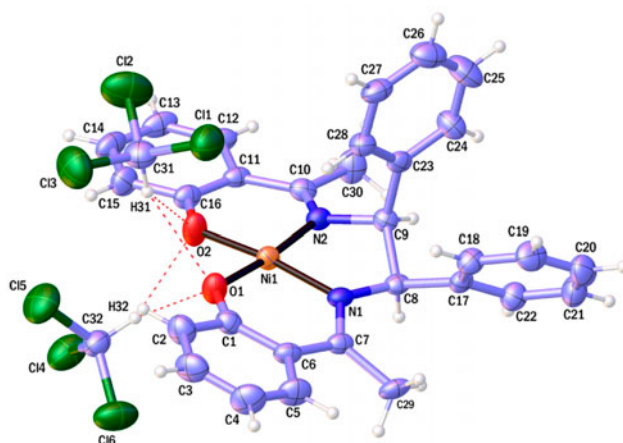


Figure 2. ORTEP representation of $\text{NiL}^4 \cdot 2\text{CHCl}_3$. Thermal ellipsoids are drawn at the 50% probability level, while the hydrogen size is arbitrary.

atom numbering scheme. All interatomic distances can be considered as normal and a summary of the crystallographic data, selected bond lengths, and bond angles are listed in tables 1 and 2. The neutral species contains one Ni(II) ion connected to the doubly deprotonated ligand (L^3)²⁻. As can be seen from table 2, both of the N(1)–Ni–N(2) and O(1)–Ni–O(2) bond angles deviate from and are smaller than the ideal 90° whereas the cisoid N–Ni–O angles are both larger than 90°. The transoid N–Ni–O angles are also both smaller than 180° causing a slightly distorted square planar geometry around the metal center, which is similar to previously reported analogue [17, 36, 37]. The angle between the two NCCCO chelating ring systems is only 2.59(3)°, which indicates a flat arrangement around the metal center. The metal atom is well located at the center of the N_2O_2 coordination sphere with the average Ni–N bond distance of 1.838 Å compared to the average Ni–O bond distance of 1.848 Å. No important hydrogen bond or π – π stacking was observed for this complex.

3.2.1. Description of the crystal structure of NiL^4 . The geometry around the metal center in the crystal structure of NiL^4 is similar to that of NiL^3 in which the geometry is distorted square planar where the N_2O_2 donating atom of the tetradentate Schiff base ligand forms the coordination sphere. The angle between the two NCCCO chelating ring systems is 15.28(2)°, which indicates more distortion towards the tetrahedral geometry. The average Ni–O bond length (1.820 Å) is shorter than the average Ni–N bond distance (1.866 Å), which confirms more distortion. Figure 2 shows the ORTEP representation of NiL^4 . As can be seen in figure 2, two CHCl_3 molecules have hydrogen bonds with both oxygen atoms of the ligand.

Table 3. Redox potential data for 10^{-3} M L^{-1} solutions of NiL^x ($x = 1-4$) complexes in DMSO solutions containing 0.1 M L^{-1} TOAB and scan rate 100 mV s^{-1} . Data are in volts.

Complex	E_{pa}	E_{pc}	E^0	ΔE
NiL^1	-1.40	-1.50	-1.45	0.10
NiL^2	-1.36	-1.41	-1.38	0.05
NiL^3	-0.98	-1.07	-1.02	0.09
NiL^4	-1.49	-1.56	-1.52	0.07

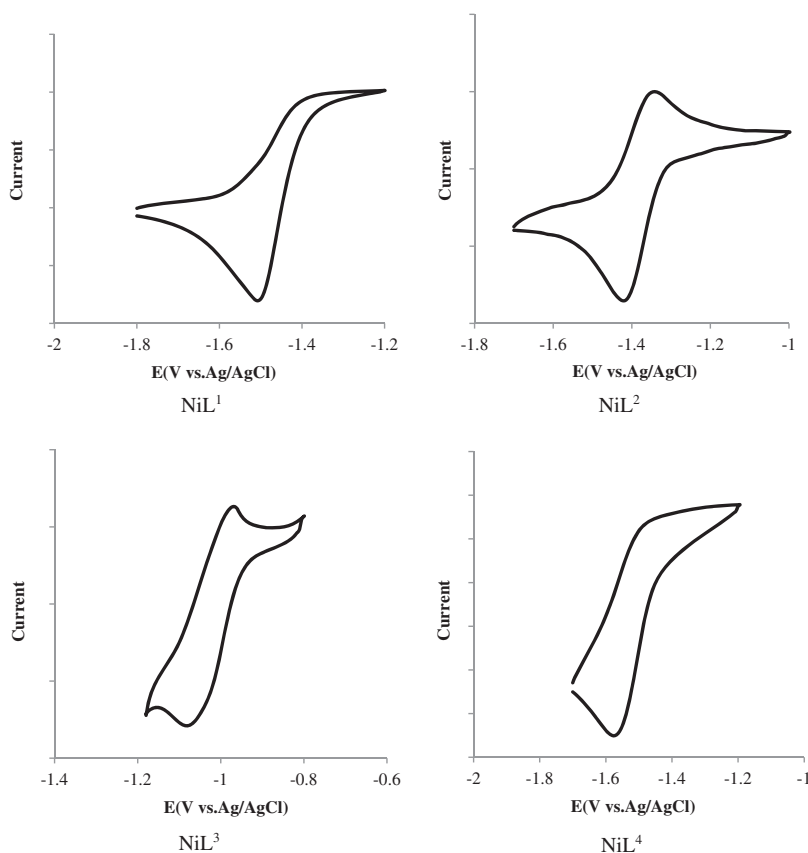
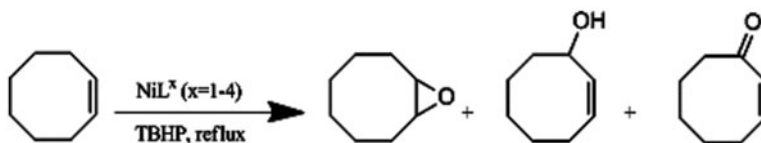


Figure 3. Cyclic voltammogram of NiL^x complexes in DMSO at 298 K and 100 mV s⁻¹ scan rate.

3.3. Electrochemistry

Electrochemical studies of the complexes were performed by means of cyclic voltammetry in the potential range of 0 to -2 volts. The CVs were obtained in DMSO solutions at room temperature (298 K) under nitrogen atmosphere using 0.1 M tetra-*n*-octylammonium bromide (TOAB) as supporting electrolyte. A platinum working electrode, a platinum auxiliary electrode, and an Ag/AgCl reference electrode was used to obtain cyclic voltammograms. The data for the complexes are collected in table 3 and the cyclic voltammogram of the NiL^x complex is shown in figure 3. The ligands were electro-inactive in the studied potential range. In the cyclic voltammogram of the NiL complexes, a reversible (for NiL²) or a quasi-reversible (for NiL^{1,3,4}) reduction wave due to Ni^{II}/Ni^I reduction process was observed, which are in good agreement with previously reported analogues [39, 40]. As can be seen from table 3, the presence of electronegative substituents on the ancillary ligands has shifted the Ni^{II}/Ni^I redox potential to less negative values and NiL³ with two electron withdrawing substituents on the salicylaldehyde moiety has the least negative value while NiL⁴ without electron withdrawing substituents and with electron donating CH₃ substituents on the ancillary ligand has the most negative reduction potential.



Scheme 2. Products of the catalytic oxidation of cyclooctene with the NiL^x catalysts and TBHP oxidant.

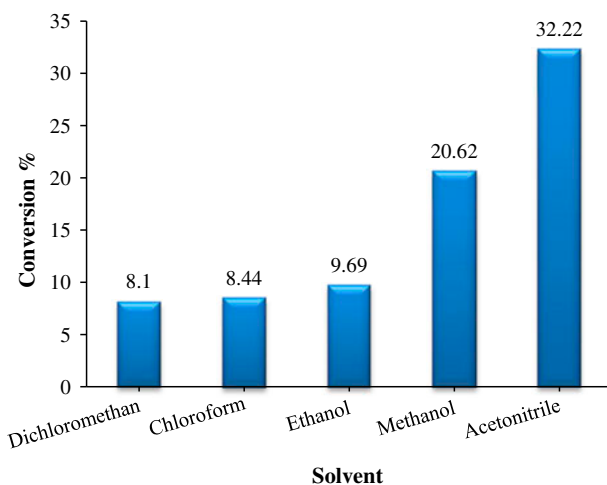


Figure 4. The results for the optimization of solvent type for NiL^4 . Reaction conditions: 15 μM of NiL^4 , 10 mL of solvent, 15 mM of cyclooctene, 45 mM of TBHP, reflux for 24 h.

3.4. Catalytic studies

3.4.1. In-solvent catalytic oxidation of cyclooctene. The catalytic oxidation of cyclooctene with these new catalysts gave three products (scheme 2). Various reaction conditions including reaction time, temperature, solvent type, catalyst type, solvent amount, amount of catalyst, and oxidant to substrate ratio were optimized. In a typical experiment, 10 μM of NiL^4 catalyst was dissolved in 10 mL of freshly distilled acetonitrile and then 15 mM of cyclooctene and 30 mM of TBHP were added. The reaction mixture was refluxed while being stirred and the reaction progress was monitored at 30 min intervals up to 30 h and 24 h was found to be the optimized reaction time. To optimize the solvent type, similar reactions were performed in five different solvents including dichloromethane, chloroform, methanol, ethanol, and acetonitrile. The results are shown in figure 4 and as can be seen, acetonitrile was chosen as the best solvent. The substrate to oxidant ratio (1 : 3), catalyst amounts (15 μM), and the reaction temperature (80 $^\circ\text{C}$) were also optimized. Then the effect of the catalyst type was studied using the above-mentioned reaction conditions. Figure 5 shows the results of the optimization of the catalyst type and as can be seen, NiL^4 was the most efficient catalyst in this process. Table 4 shows the results of the catalytic data at optimized conditions for different catalysts. It can be concluded from the comparison of tables 3 and 4 that there is a good correlation between the catalytic performances of the complexes with their redox potential. NiL^4 with more electron donating substituents on the ligand has the most negative E^0 and was the most efficient oxidation catalyst while NiL^3 with more

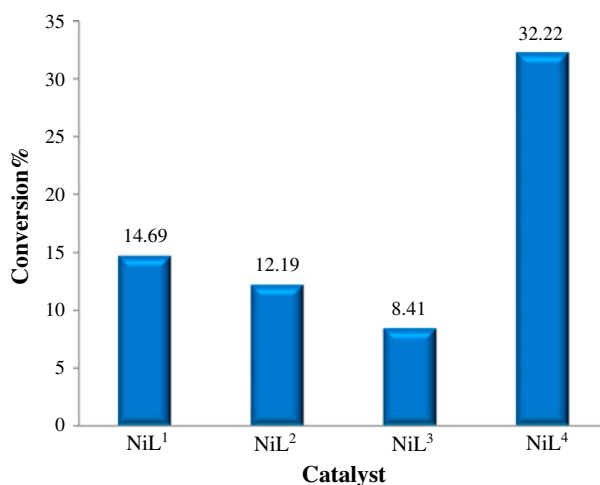


Figure 5. The results of the catalytic oxidation of cyclooctene with NiL¹⁻⁴. Reaction conditions: 15 μ M of NiL^x (x = 1-4), 10 mL of freshly distilled acetonitrile, 15 mM of cyclooctene, 45 mM of TBHP, reflux for 24 h.

Table 4. Oxidation of cyclooctene with TBHP in the presence of NiL^x (x = 1-4) in optimized reaction conditions.

Complex	Conversion %	Turn over number (TON)	Selectivity		
					
NiL ¹	14.69	147	44.56	15.99	39.45
NiL ²	12.19	122	50.08	16.28	33.64
NiL ³	8.41	84	51.24	19.37	29.39
NiL ⁴	32.22	322	42.93	25.22	31.85

Table 5. Oxidation of cyclooctene with TBHP in the presence of NiL^x (x = 1-4) in solvent-free conditions.

Complex	Conversion %	Turn over number (TON)	Selectivity		
					
NiL ¹	36.88	369	63.35	18.64	18.00
NiL ²	36.51	365	64.10	13.09	22.81
NiL ³	30.16	302	74.88	11.09	14.03
NiL ⁴	42.47	425	69.26	18.56	11.88

electron withdrawing substituents on the ligand and with the most positive E^0 value was the least active catalyst. Considering the epoxide selectivity on the other hand, NiL³ with more electron withdrawing substituents showed higher selectivity. Although the electrochemistry and electronic effects of the substituents are important factors, more work is necessary to be done to find all the effects governing such reactivity. Our data are comparable with the results of the oxidation of cyclooctene using nickel(II) Schiff base complexes found in the literature [23-25].

3.4.2. Solvent-free catalytic oxidation of cyclooctene. Similar catalytic experiments were performed with NiL^x catalysts in the solvent-free conditions. To compare the results, we used the optimized catalytic conditions mentioned for in-solvent oxidation reactions. A similar trend was observed and NiL^4 was found again to be the most efficient oxidation catalyst with highest conversion percentage and NiL^3 was the least active one. Considering the epoxide selectivity, NiL^3 was again the most selective catalyst. Besides, increased catalytic activity and higher epoxide selectivity was observed for all of the complexes in our solvent-free studies compared to in-solvent conditions (table 5).

4. Conclusion

Three new and one previously reported Ni(II) complexes of salen type Schiff base ligands were synthesized and characterized by spectroscopic methods as well as elemental analysis and X-ray crystallography. Catalytic performances of these complexes were studied both in solvent and solvent-free conditions and several factors affecting the catalytic activity of the complexes were optimized. Although high-valent complexes such as Mo^{VI} [16, 28], W^{VI} [29], or V^{IV} [24] Schiff bases are reported to be highly active epoxidation catalysts, a literature survey shows that some lower valent complexes are also active in this reaction [26, 38]. Indeed, the oxidation number is not the only factor affecting the epoxidation efficiency of the catalyst and other factors need to be studied and still more work is necessary to find all factors governing such reactivity. In our research group, we are studying the effect of different metal ions with similar Schiff base ligands on epoxidation performance and selectivity, as well as the study of other important variables. In this work, we report the results of our studies using nickel(II) Schiff base complexes as catalysts. Our complexes showed almost similar activity (conversion percent) and epoxide selectivity compared to many other Ni(II) Schiff bases. But we were able to achieve higher epoxide selectivity compared to several previously reported Ni(II) Schiff base complexes in our solvent-free conditions [17, 20].

Supplementary material

CCDC 941409 and 941410 contains the supplementary crystallographic data for NiL^3 and NiL^4 , respectively. These data can be obtained free of charge via <http://www.ccdc.cam.ac.uk/conts/retrieving.html>, or from the Cambridge Crystallographic Data Centre, 12 Union Road, Cambridge CB2 1EZ, UK; fax: (+44) 1223-336-033; or e-mail: deposit@ccdc.cam.ac.uk.

Acknowledgement

We are acknowledged to the office of gifted students at Semnan University for financial supports.

References

- [1] A.H. Kianfar, L. Keramat, M. Dostani, M. Shamsipur, M. Roushani, F. Nikpour. *Spectrochim. Acta Part A*, **77**, 424 (2010).
- [2] S. Zolezzi, E. Spodine, A. Decinti. *Polyhedron*, **21**, 55 (2002).
- [3] F. Zaera. *J. Mol. Catal. A Chem.*, **228**, 21 (2005).

- [4] M. Peters, R. Breinbauer. *Tetrahedron Lett.*, **51**, 6622 (2010).
- [5] E.G. Jäger, K. Schuhmann, H. Görls. *Inorg. Chim. Acta*, **255**, 295 (1997).
- [6] J.A.L. da Silva, J.J.R. Fraústo da Silva, A.J.L. Pombeiro. *Coord. Chem. Rev.*, **255**, 2232 (2011).
- [7] J. Costamagna, J. Vargas, R. Latorre, A. Alvarado, G. Mena. *Coord. Chem. Rev.*, **119**, 67 (1992).
- [8] M. Salavati-Niasari. *J. Mol. Catal. A Chem.*, **263**, 247 (2007).
- [9] V. Mirkhani, S. Tangestaninejad, M. Moghadam, I. Mohammadpoor-Baltork. *H. Kargar*, **242**, 251 (2005).
- [10] A.H. Sarvestani, A. Salimi, S. Mohebbi, R. Hallaj. *J. Chem. Res.*, **190** (2005).
- [11] K.C. Gupta, A.K. Sutar. *Coord. Chem. Rev.*, **252**, 1420 (2008).
- [12] M. Bagherzadeh, M. Zare. *J. Coord. Chem.*, **66**, 2885 (2013).
- [13] A. Aghmiz, N. Mostfa, S. Iksi, R. Rivas, M.D. González, Y. Díaz, F. El Guemmout, A. El Laghdach, R. Echarrí, A.M. Masdeu-Bultó. *J. Coord. Chem.*, **66**, 2567 (2013).
- [14] E.N. Jacobsen, W. Zhang, A.R. Muci, J.R. Ecker, L. Deng. *J. Am. Chem. Soc.*, **113**, 7063 (1991).
- [15] S. Bunce, R.J. Cross, L.J. Farrugia, S. Kunchandy, L.L. Meason, K.W. Muir, M.O. Donnell, R.D. Peacock, D. Stirling, S.J. Teat. *Polyhedron*, **17**, 4179 (1998).
- [16] Y.-M. Cui, Y. Wang, Y.-J. Cai, X.-J. long, W. Chen, *J. Coord. Chem.*, **66**, 2325 (2013).
- [17] Y. Huang, T. Liu, J. Lin, J. Lü, Z. Lin, R. Cao. *Inorg. Chem.*, **50**, 2191 (2011).
- [18] M. Salavati-Niasari, M. Hasani-Kabutarikhani, F. Davar. *Catal. Commun.*, **7**, 955 (2006).
- [19] S. Bhunia, S. Koner. *Polyhedron*, **30**, 1857 (2011).
- [20] D. Chatterjee, S. Mukherjee, A. Mitra. *J. Mol. Catal. A Chem.*, **154**, 5 (2000).
- [21] A. Ghaffari, M. Behzad, G. Dutkiewicz, M. Kubicki, M. Salehi. *J. Coord. Chem.*, **65**, 840 (2012).
- [22] D.M. Boghaei, A. Bezaatpour, M. Behzad. *J. Coord. Chem.*, **60**, 973 (2007).
- [23] J. Rahchamani, M. Behzad, A. Bezaatpour, V. Jahed, G. Dutkiewicz, M. Kubicki, M. Salehi. *Polyhedron*, **30**, 2611 (2011).
- [24] A. Bezaatpour, M. Behzad, D.M. Boghaei. *J. Coord. Chem.*, **62**, 1127 (2009).
- [25] S.-B. Ding, W.-H. Li. *J. Coord. Chem.*, **66**, 2023 (2013).
- [26] A. Banaei, B. Rezazadeh. *J. Coord. Chem.*, **66**, 2129 (2013).
- [27] R. Klement, F. Stock, H. Elias, H. Paulus, P. Pelikán, M. Valko, M. Mazür. *Polyhedron*, **18**, 3617 (1999).
- [28] X.-Q. He. *J. Coord. Chem.*, **66**, 966 (2013).
- [29] M. Amini, M. Bagherzadeh, B. Eftekhari-Sis, A. Ellern, L.K. Woo. *J. Coord. Chem.*, **66**, 1897 (2013).
- [30] M. Bagherzadeh, M. Zare. *J. Coord. Chem.*, **65**, 4054 (2012).
- [31] M.N.H. Irving, R.M. Parkins. *J. Inorg. Nucl. Chem.*, **27**, 270 (1965).
- [32] L.N. Rusere, T. Shalumova, J.M. Tanski, L.A. Tyler. *Polyhedron*, **28**, 3804 (2009).
- [33] (a) COSMO, version 1.60, Bruker AXS Inc., Madison, WI, USA (2005); (b) SAINT, version 7.06A, Bruker AXS Inc., Madison, WI, USA (2005); (c) SADABS, version 2.10, Bruker AXS Inc., Madison, WI, USA, (2005).
- [34] M.C. Burla, R. Caliendo, M. Camalli, B. Carrozzini, G.L. Cascarano, L. De Caro, C. Giacovazzo, G. Polidori, R. Spagna. *J. Appl. Crystallogr.*, **38**, 381 (2005).
- [35] G.M. Sheldrick. *SHELXL-97*, University of Göttingen, Göttingen, Germany (1997).
- [36] G. Hoshina, M. Tsuchimoto, S. Ohba. *Acta Cryst.*, **C56**, e122 (2000).
- [37] M. Mariappan, M. Suenaga, A. Mukhopadhyay, B.G. Maiya. *Inorg. Chim. Acta*, **390**, 95 (2012).
- [38] M.R. Maurya, P. Saini, C. Haldar, A.K. Chandrakar, S. Chand. *J. Coord. Chem.*, **65**, 2903 (2012).
- [39] M.H. Habibi, R. Mokhtari, M. Mikhak, M. Amirasr, A. Amiri. *Spectrochim. Acta Part A*, **79**, 1524 (2011).
- [40] E. Dunach, A.P. Esteves, M.J. Medeiros, D. Pletcher, S. Olivero. *J. Electroanal. Chem.*, **39**, 566 (2004).